Localization of *Xcat*-2 RNA, a putative germ plasm component, to the mitochondrial cloud in *Xenopus* stage I oocytes

Yi Zhou[†] and Mary Lou King*

Department of Cell Biology and Anatomy (R-124), University of Miami School of Medicine, Miami, FL 33136, USA

*Author for correspondence (e-mail: mking@mednet.med.miami.edu)
†Present address: Children's Hospital, Hematology/Oncology Laboratory, 300 Longwood Avenue, Boston, MA 02115-5737, USA

SUMMARY

The mitochondrial cloud is a unique cell structure found in stage I *Xenopus* oocytes that plays a role in mitochondriogenesis and in the distribution of germ plasm to the vegetal pole. *Xcat*-2 RNA specifically localizes to the mitochondrial cloud and moves with it to the vegetal subcortex in stage II oocytes. Later, in the 4-cell embryo, it is found in a pattern identical to the germ plasm. Following microinjection into stage I oocytes, synthetic *Xcat*-2 RNAs localize to the mitochondrial cloud within 22 hours. Transcripts are stable over this time period with very little evidence of degradation. The *Xcat*-2 3′untranslated region was found to be both required and sufficient for mitochondrial cloud localization. Further deletion analysis narrowed this localization signal to a 250 nucleotide region at the proximal end of the 3′untranslated region. This region is different from, but overlaps with, a domain previously shown to be sufficient to direct *Xcat*-2 to the vegetal cortex in stage IV oocytes. Examination of early stage I oocytes reveals a time when *Xcat*-2 is uniformly distributed, arguing against vectorial nuclear export into the mitochondrial cloud. Analysis of localization at different time points does not suggest active transport to the mitochondrial cloud. We postulate that localization occurs by selective entrapment of *Xcat*-2 within the cloud by localized binding sites.

Key words: *Xenopus*, localized maternal mRNA, germ plasm, mitochondrial cloud, *Xcat*-2, oocyte

INTRODUCTION

In previtellogenic oocytes, a 'necklace' consisting of small clusters of mitochondria surround the nucleus or germinal vesicle (GV) (Dumont, 1972; Heasman et al., 1984). One cluster, on the centriolar side of the GV, becomes distinctly larger (20-40 μm in diameter) than the others and is called the mitochondrial cloud (Billet and Adam, 1976). Later during oogenesis, it is evident that the mitochondrial cloud marks the basal or vegetal pole side of the GV. The mitochondrial cloud is a site of intense mitochondriogenesis and, together with the other clusters, constitutes the impressive maternal contribution of this organelle to the embryo (Tourte et al., 1984).

Several unique features distinguish the mitochondrial cloud from the other perinuclear mitochondrial aggregates. The mitochondrial cloud has a distinct cytoarchitecture and retains its integrity when removed from the cell with a micropipette. Immunohistochemical staining reveals microtubules and intermediate filaments surrounding as well as penetrating the cloud (Wylie et al., 1985a; Gard et al., 1995). Disruption of microtubules leaves the mitochondrial cloud intact while the perinuclear clumps disaggregate (Heasman et al., 1984). Besides Golgi complexes, lipid and smooth endoplasmic reticulum, the mitochondrial cloud is also the exclusive site of germ plasm, a distinctive association of mitochondria, lipid and germinal granules. These granules contain RNA and protein and evidence strongly supports their role as determinants of the germ cell lineage (Mahowald and Hennen, 1971; Ikenishi et al., 1986; Heasman et al., 1984). At the beginning of stage II, the mitochondrial cloud fragments, and at least half of it moves down and into the vegetal cortex. Based on these observations, another major function of the mitochondrial cloud, besides mitochondriogenesis, has been proposed: i.e. to concentrate and to distribute the germ plasm to the vegetal pole where it is eventually inherited by the primordial germ cells (Heasman et al., 1984).

At least two pathways have been identified for localizing RNAs to the vegetal cortex in *Xenopus* (King, 1995; Forristall et al., 1995). One occurs early during stage I/II, the other functions later, during stage III/IV. Several RNAs, including *Xlsirt* (Kloc et al., 1993), *Xwnt*-11 (Kloc and Etkin, 1995) and *Xcat*-2 mRNA (Forristall et al., 1995), have been mapped to the mitochondrial cloud by in situ hybridization and these RNAs move with the cloud material to the vegetal cortex early in oogenesis. *Vg*1 localizes much later in stage IV oocytes (Yisraeli and Melton, 1988; Forristall et al., 1995). Movement of *Vg*1 requires intact microtubules and most likely is actively transported to the cortex (Yisraeli et al., 1990).

It is unknown how *Xcat*-2 RNA concentrates within the mitochondrial cloud, although its localization is of special interest as it appears to be a component of the germ plasm (Forristall et al., 1995). Understanding the mechanism of *Xcat*-2 localization may shed some light on the ontogeny of the germ

plasm and hence germ cell specification. *Xcat*-2 encodes a putative zinc finger RNA-binding protein related to the *Drosophila* determinant *nanos* (Mosquera et al., 1993). Interestingly, *nanos* is also inherited by the germ plasm in pole cells (Wang et al., 1994) and is required for germ-line development. In *nanos* mutants, pole cells fail to migrate into the gonads (Kobayashi et al., 1996) and females lay few eggs (Lehmann and Nusslein-Volhard, 1991).

Besides active microtubular based transport, there are several other possible mechanisms to be considered for localizing *Xcat*-2. For example, hsp83 RNA is localized to the posterior pole of *Drosophila* oocytes by selective protection there and widespread degradation everywhere else (Ding et al., 1993). RNAs may accumulate at a specific site because of specific 'receptors' being localized there as has been suggested for *nanos* (Wang et al., 1994) and cyclin B RNAs (Raff et al., 1990). Yet another mechanism, vectorial nuclear transport, has been proposed for some pair-rule genes in *Drosophila* (Davis and Ish-Horowicz, 1991). In all these examples of RNA localization, sequences in the 3′UTR are required to mediate the process (reviewed in St Johnston, 1995).

Here we have analyzed *Xcat*-2 localization to the mitochondrial cloud by injecting tagged synthetic RNAs into stage I oocytes. The minimum *cis*-localization elements required and sufficient for *Xcat*-2 localization were mapped and include part of a smaller domain required for cortical localization (Zhou and King, 1996). Analysis of localization at different time points is most consistent with a model where *Xcat*-2 is sequestered within the cloud by localized binding sites.

MATERIALS AND METHODS

Oocytes, oocyte injection and oocyte culture

Stage I oocytes (50-250 μm in diameter) were dissected from an adult or juvenile ovary and defolliculated using 0.15% collagenase B (Boehringer Mannheim) as previously described (Forristall et al., 1995). Oocytes were maintained in 1× MBSH (Gurdon, 1968; Peng, 1991) supplemented with 100 unit/ml of penicillin and 100 μg/ml streptomycin prior to injection of transcripts.

Approximately 10-50 pg of a given transcript was injected into mature stage I oocytes in a volume of 0.5 nl using a Narishige PC-3000 microinjector. Oocytes were washed three times in 1× MBSH containing antibiotics and cultured in 0.5× Leibowitz medium supplemented with 1 mM L-glutamine, 1 μg/ml insulin, 15 mM Hepes (pH 7.8), 50 units/ml nystatin, 100 μg/ml gentamicin and 10% frog serum containing vitellogenin or 10% fetal calf serum (Wallace et al., 1980; Yisraeli and Melton, 1988). Oocytes were incubated at 20°C in a humidified chamber for up to 24 hours.

DNA manipulation and in vitro transcription

The LrRNA cDNA clone contains 650 nt (79-708 nt) of the mitochondrial large ribosomal RNA gene in pBluescript (Yost et al., 1995). LrRNA served as a marker for the mitochondrial cloud. The original *Xcat*-2 clone in pSPORT is described in Mosquera et al. (1993). The construct pNB40 *Xcat*-2 was a gift from Drs R. Lehmann and C. Wang and contained a 50 nt *Xenopus* β-globin mRNA leader sequence fused to the 5′ end of full-length *Xcat*-2. The XβG-340/3′ clone was a gift from Dr K. Mowry (Mowry and Melton, 1992). XβG-340/3′ contains the *Xenopus* β-globin-coding sequence fused to the *Vg*1 340 nt localization signal. ODC2 (ornithine decarboxylase) was a gift from Dr C. Wright (Bassez et al., 1990).

The deletion mutants tagged with the *Xenopus* β-globin 5′ leader sequence were constructed as follows. The *Xcat*-2 open reading frame

(5′ORF) was isolated from pNB*Xcat*-2 as a *Mlu*I-*Bst*NI 470 bp fragment and ligated into the pNB40 vector at *Mlu*I and *Not*I sites. The *Xcat*-2 3′untranslated region (410 bp 3′UTR) was released from pNB*Xcat*-2 after *Dde*I and *Not*I digestion and ligated into the pNB40 vector at *Mlu*I and *Not*I sites. The *Hin*dIII-*Sma*I 310 bp fragment from the 3′UTR clone was ligated into the pNB40 vector at the *Hin*dIII and *Not*I sites to make 3′UTRΔ1, a mutant lacking the terminal half of the 3′UTR. 3′UTRΔ2, missing the proximal half of the 3′UTR, was constructed by removing the *Sma*I-*Mlu*I fragment from the 3′UTR clone and religating the ends. 3′UTRΔ3, missing the middle portion of the 3′UTR sequence was created by releasing the *Bcl*I-*Apa*I (blunt-ended by nuclease) fragment from the 3′UTR clone and religating the clone. The *Bcl*I-*Apa*I fragment was ligated into the pNB40 vector at *Mlu*I and *Not*I sites to create 3′UTRΔ4, containing only the middle portion of the 3′UTR.

The 3′UTR of *Xcat*-2 was inserted between the *Sal*I and *Not*I sites in the pSPORT vector (BRL). Luciferase-tagged 3′UTR-*Xcat*-2 was produced by ligating pT3/T7-luc (Clonetech) vector fragments, *Kpn*I-*Nde*I and *Nde*I-*Sma*I, with the 3′UTR of *Xcat*-2 bearing *Kpn*I and blunt-ends from the pSPORT3′UTR construct. Deletion of a 1.5 kb portion of the luciferase insert between two *Bsp*MI sites produced a 413 nt luciferase fragment ligated to the 3′UTR of *Xcat*-2 (Luc/3′UTR). A vector (pT3/T7-luc3′) containing the 413 nt fragment from the 3′ end of the luciferase-coding region (1479-1892) was made from the pT3/T7-luc clone by simply deleting the region between two *Bsp*M1 sites. Mutant constructs are diagrammed in Fig. 4.

To make transcription templates, XβG-340/3′ was linearized with *Eco*RI and transcribed with SP6 RNA polymerase to produce 850 nt transcripts. pNB40*Xcat*-2, 5′ORF, 3′UTR, 3′UTRΔ1, 3′UTRΔ2, 3′UTRΔ3 and 3′UTRΔ4 were all linearized with *Pvu*II and transcribed with SP6 RNA polymerase to produce 850 nt, 460 nt, 460 nt, 370 nt, 280 nt, 370 nt and 250 nt transcripts respectively. Luc/3′UTR, was linearized with *Xho*I and transcribed with T3 RNA polymerase to produce a 870 nt transcript. All transcripts were capped and then polyadenylated by using recombinant yeast poly(A) polymerase (Rusconi and Flick, 1993).

Probes and RNase protection

For RNase protection assays, pNB40*Xcat*-2 and 5′ORF probe constructs were made by deleting the region between two unique sites, *Sac*II and *Not*I in the 5′ORF clone, treating with Mungbean nuclease and blunt end ligating the 2,620 nt fragment together. This clone contained the 50 nt *Xenopus* β-globin mRNA leader sequence and 144 nt 5′-end fragment of *Xcat*-2 clone in the pNB40 vector.

RNase protection assays were performed essentially as described by Melton et al. (1984) with a few modifications as outlined in Forristall et al. (1995). *Hin*dIII digestion of a pNB40 *Xcat*-2 subclone yielded a probe of approximately 210 nucleotides after T7 RNA polymerase transcription. This probe resulted in a protected fragment of 144 nt for endogenous *Xcat*-2. The probe for *Vg*1 was transcribed from linearized pSPT73XβG5′ plasmid, a gift of Dr Kim Mowry (Mowry and Melton, 1992) by SP6 RNA polymerase. The resulting probe was about 400 nt in size and protected a major 262 nt fragment, but also resulted in multiple bands as shown previously (Melton, 1987). A probe for ODC (ornithine decarboxylase) was used as a control for RNA loading and protected a 90 nt fragment (Bassez et al., 1990).

In situ hybridization and autoradiography

Non-radioactive in situ hybridizations were done according to the protocol developed by Oberman and Yisraeli (1995) and Harland (1991) with a few modifications. Defolliculated oocytes were fixed in 0.25% chromium trioxide in 95% ethanol and 5% acetic acid at 4°C for 1 hour. Paraffin sections were cut at 5 μm. Dewaxed, rehydrated sections were refixed in 4% paraformaldehyde for 20 minutes and then pretreated at 37°C for one to two minutes with a proteinase K solution (1.5 μg/ml in 0.1 M Tris-HCl, pH 7.5, 0.01 M EDTA; Solution proteinase K was purchased from BMB). Slides were then washed in 0.2 M HCl and 0.1 M triethanolamine pH 8.0 with 0.25% acetic anhydride,

dehydrated in a graded ethanol series and air dried at room temperature. PEP-PEN (Electron Microscopy Science) was used to create a water-impermeable barrier around the sections in order to avoid using coverslips in later steps. After 1 hour of prehybridization, hybridization solution (50% formamide, 10% dextran sulfate, 0.3% NaCl, 10 mM Tris-HCl, pH 8.0, 2 mM EDTA, 1× Denhardts, 0.1% CHAPS, and 0.1% Tween 20) containing denatured *Xcat*-2 (1 µg/ml) or LrRNA (0.2 µg/ml) probes were added and hybridization proceeded overnight at 45°C. All in situ hybridizations were done with digoxigenin (DIG, Boehringer Mannheim) labeled probes. At the end of the hybridization period, slides were washed in 2× SSPE, 0.1% CHAPS for 30 minutes at room temperature, treated with RNase A (20 µg/ml) in 4× SSPE with 0.1% CHAPS for another 30 minutes and finally washed in 0.1× SSPE at room temperature for 5 minutes. Prior to immunodetection of the probe, slides were washed in 1× PBS, 0.1% Tween-20 for 10 minutes followed by PBT (1× PBS, 2 mg/ml BSA, 0.1% Triton X-100) for 15 minutes. Slides were then covered with a solution of 20% fetal calf serum in PBT containing a 1:1000 dilution of the affinity-purified sheep anti-digoxigenin antibody coupled to alkaline phosphatase (BMB). Anti-DIG antibody incubations were carried out either at room temperature for 4 hours or at 4°C overnight. Excess antibody was removed by four 5 minute washes in PBT at room temperature. The chromogenic reaction employed BM purple AP as substrate (BMB). Slides were treated at room temperature until a signal appeared. The reaction was stopped with 10 mM Tris-HCL, 1 mM EDTA, pH 7.5. Samples were then dehydrated in a graded ethanol series to 100% xylene and mounted in Paramount (Sigma).

For autoradiographic analysis, ^{35}S-labelled, capped and polyadenylated transcripts with specific activities around 5×10^7 dpm/µg (Krieg and Melton, 1984; Rusconi and Flick, 1993) were microinjected into stage I oocytes and the oocytes cultured, fixed and sectioned as described above. Slides were dipped in Kodak NBT-2 emulsion diluted with NH$_4$OAc as instructed by the company and air dried. Exposure times were for 1-3 weeks.

Computer modeling

A direct comparison was made of the nucleotide sequences of the RNA localization signal (RLS) from *Xcat*-2, *Xlsirt*, *Xwnt*-11 and *Vg*1 using the University of Wisconsin GCG programs COMPARE and BESTFIT. RNA secondary structures were generated by using the energy minimization methods of Zuker (1989). Mfold and FoldRNA functions of GCG (Genetic Computer Group) program were employed.

RESULTS

Xcat-2 mRNA localizes exclusively to the mitochondrial cloud in stage I oocytes

Previous work has shown that *Xcat*-2 RNA is concentrated within the mitochondrial cloud present in stage I oocytes (Forristall et al., 1995). Whether *Xcat*-2 was also associated with the smaller mitochondrial aggregates present around the nucleus remained an open question. To clarify this point, antisense RNA probes for the large mitochondrial rRNA subunit (LrRNA; Fig. 1A), *Xcat*-2 (Fig. 1B) and a mixture of both (Fig. 1C) were hybridized to serial sections of stage I oocytes (250 µm). As expected, the LrRNA

probe hybridized to the mitochondrial cloud as well as the perinuclear aggregates. *Xcat*-2 hybridized exclusively to the mitochondrial cloud. The results of hybridizing a mixture of these two probes together confirmed that the site of *Xcat*-2 localization and the mitochondrial cloud coincided; no additional structures were indicated. From this we can conclude that *Xcat*-2 mRNA localizes exclusively to the mitochondrial cloud and does not enter the mitochondrial clumps that are present at this stage. These results further indicate that the cloud is different from the other aggregates of mitochondria and must contain binding sites for *Xcat*-2.

Xcat-2 is uniformly distributed in early stage I oocytes

One question that arises from the above analysis is whether *Xcat*-2 is vectorially exported out of the nucleus directly into the closely apposed mitochondrial cloud. To address this question, we examined sections of earlier stage I oocytes by whole-mount in situ hybridization and asked if there was a time when *Xcat*-2 was not localized. Fig. 1D shows that *Xcat*-2 signal was found throughout the ooplasm of small stage I oocytes approximately 50-70 µm in diameter. RNase protection assays confirmed the presence of *Xcat*-2 RNA at these early stages (Fig. 2C). Examples of apparent intermediate stages in localization where *Xcat*-2 appeared both in the ooplasm and in the mitochondrial cloud (Fig. 1E) were also observed. These observations make it unlikely that *Xcat*-2 is
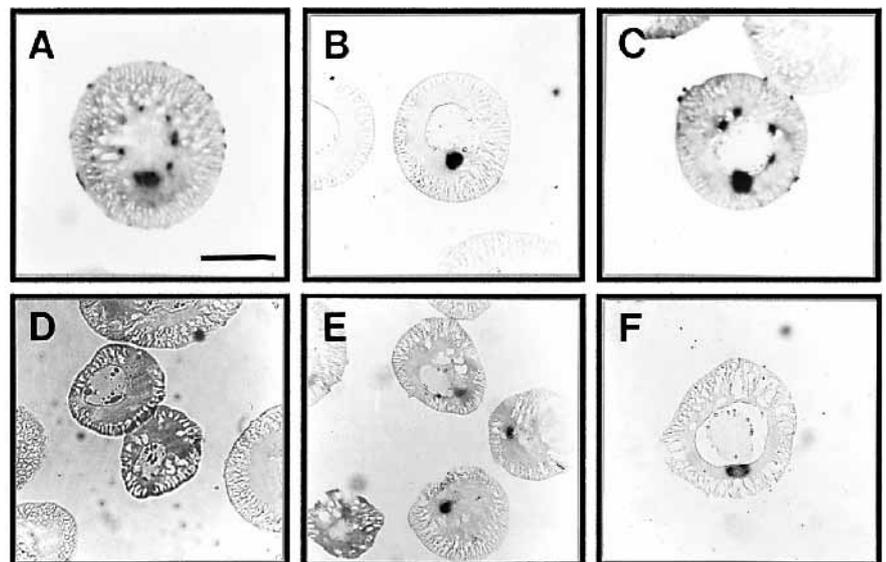

Fig. 1. *Xcat*-2 mRNA progressively localizes to and is found exclusively in the mitochondrial cloud of stage 1 oocytes. In situ hybridizations with stage 1 oocytes approximately 250 µm (A-C) or 50-70 µm (D-F) in diameter. Detection was by a digoxigenin-labeled antisense RNA probe for (A) the mitochondrial large ribosomal RNA (LrRNA), (B,D-F) *Xcat*-2 and (C) a mixture of both probes. (A) The LrRNA probe hybridizes to the mitochondrial aggregates surrounding the nucleus as well as to the large mitochondrial cloud. (B) Endogenous *Xcat*-2 RNA is present only in the mitochondrial cloud. (C) A mixture of both probes reveals that *Xcat*-2 and the mLrRNA co-localize with the mitochondrial cloud as no additional structures were detected. All oocytes shown in D-F were processed together on one slide. (D) Endogenous *Xcat*-2 in small stage I oocytes is uniformly distributed in the cell. (E) *Xcat*-2 partially localized to the mitochondrial cloud. (F) Mitochondrial cloud localization appears complete for *Xcat*-2. Bar, 80 µm.

vectorially exported out of the nucleus. A more probable explanation is that, in early stage I oocytes, *Xcat-2* is newly transcribed and distributed throughout the oocyte. As the oocyte and mitochondrial cloud develop, *Xcat-2* is localized within the cloud.

Does *Xcat-2* accumulate within the mitochondrial cloud, or is ooplasmic *Xcat-2* degraded and only that RNA within the mitochondrial cloud preserved? We examined the levels of *Xcat-2* during oogenesis by RNase protection and found that the total amount of *Xcat-2* remained constant from late stage I to stage VI oocytes (Fig. 2B). Early stage I oocytes as depicted in Fig. 1D contained a quarter of the amount found in mature stage I oocytes (Fig. 2C). In mature stage I oocytes, *Xcat-2* was never detected outside the mitochondrial cloud. Either *Xcat-2* is no longer synthesized at these stages or it is synthesized and transported rapidly into the cloud. Although we cannot rule out that rapid synthesis and degradation are taking place, it seems unlikely that degradation can account for *Xcat-2* mitochondrial cloud localization.

Injected *Xcat-2* RNA localizes to the mitochondrial cloud

Synthetic transcripts of localized RNAs have generally been found to localize correctly after injection into a cell. Does *Xcat-2* RNA contain *cis*-acting elements sufficient to target it to the mitochondrial cloud? To address this question, approximately 20 pg of ^{35}S-labeled polyadenylated and capped *Xcat-2* transcripts were injected into stage I oocytes. Transcripts were injected into the GV or on the opposite side of the nucleus from the mitochondrial cloud. Oocytes were cultured for 24 hours and localization evaluated by autoradiography. Mitochondrial clouds were identified by acid fuchsin staining and only those sectioned oocytes demonstrating a cloud were counted (Hausen and Riebesell, 1991). After 22-24 hours, the injected *Xcat-2* had concentrated within the mitochondrial cloud in 81% of the cases (Figs 3A,B, 4). *Vg*1 mRNA does not localize to the mitochondrial cloud but moves to the vegetal cortex late during stage III/IV. Until then, it is equally distributed in the ooplasm (Melton, 1987; Forristall et al., 1995). Mowry and Melton (1992) have shown that a relatively large segment of 340 nt in the *Vg*1 3′UTR is sufficient for vegetal localization at stage IV. We used the *Vg*1 transcript as a control for specificity, and found, as expected, that it did not localize to the mitochondrial cloud (Fig. 3C). Therefore, the information required to specify mitochondrial cloud localization resides within the *Xcat-2* transcript, whereas the *Vg*1 3′UTR vegetal signal cannot target *Vg*1 to the cloud. Furthermore, the anchoring sites for *Xcat-2* in the mitochondrial cloud must be in excess as injected transcript levels were twofold to fivefold over endogenous and were still localized.

To assess the time periods involved in localization, oocytes were also examined after 4 and 8 hours of culture. Neither time period was sufficient for localization to be completed, indicating that injected transcripts were not rapidly translocated into the cloud material. The pattern of localization was also informative. In contrast to what is observed for *Vg*1 localization, *Xcat-2* signal declines uniformly throughout the ooplasm and concentrates within the cloud exclusively. We never observed a perinuclear localization for *Xcat-2* or *Xcat-2* in transit moving up a concentration gradient; two steps typically observed during the active transport of *Vg*1 to the vegetal cortex in stage III/IV oocytes (Fig. 3A,B,E). These observa-

tions are most consistent with an entrapment model for *Xcat-2* mitochondrial cloud localization.

The 3′UTR of *Xcat-2* is both required and sufficient for mitochondrial cloud localization

Localization elements for RNAs have invariably mapped to regions within the 3′UTR (MacDonald and Struhl, 1988; Wang et al., 1994; MacDonald et al., 1993, Kim-Ha et al., 1993; Kislauskis et al., 1994; Mowry and Melton, 1992) with sizes varying from 53 (β-actin in fibroblast cells) to 630 nt (*Drosophila* bicoid) in length. As a first step in mapping the
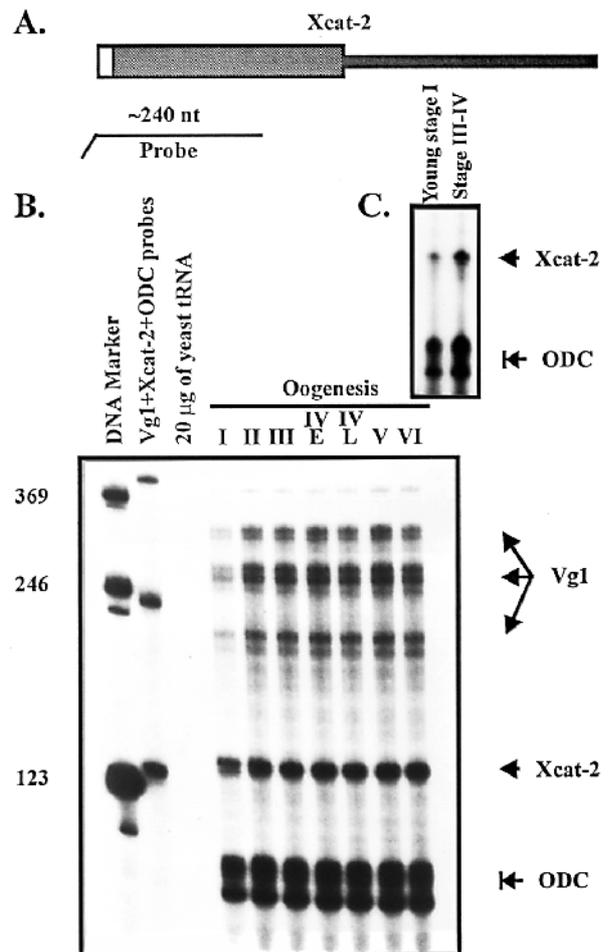

Fig. 2. Endogenous *Xcat-2* levels remain constant throughout oogenesis. The concentration of *Xcat-2* and *Vg*1 in stage I, II, III, IV early (E), IV late (L), V and VI oocytes was determined by RNase protection. The steady state level of *Xcat-2* remains the same throughout oogenesis, arguing against RNA degradation as a mechanism for mitochondrial cloud localization. (A) Diagram of *Xcat-2* mRNA with 5′ leader (open box), coding region (shaded box), 3′UTR (thick line). (B) RNase protection. Two oocyte-equivalents were loaded per lane. The probes used were *Vg*1 (~400 nt), *Xcat-2* (240 nt) and ODC (120 nt) as indicated. Note that *Xcat-2* appears to accumulate before *Vg*1 does in late stage I oocytes. The *Vg*1 antisense probe is protected from RNase digestion by *Vg*1 transcripts to give multiple bands as shown previously (Rabagliati et al., 1985; Melton, 1987). ODC (ornithine decarboxylase) was used as a control for RNA loading (Bassez et al., 1990) and yeast total RNA (20 µg) was used as a control for specificity. (C) RNase protection showing *Xcat-2* is present in young oocytes (50-70 µm; as in Fig. 1D) and increases in amount in late stage I oocytes (250 µm) relative to the ODC control.

Fig. 3. *Xcat*-2 RNA, but not *Vg*1 RNA, contains a signal required and sufficient for mitochondrial cloud localization. (A-E) Oocytes were injected with ^{35}S-labeled *Xcat*-2 or XβG-340/3′ transcripts on the side opposite the mitochondrial cloud (A,B) 22 hours after injection, *Xcat*-2 is localized within the mitochondrial cloud whereas (C) the *Vg*1 XβG-340/3′ transcript remains unlocalized. (D) The *Xcat*-2 5′ORF fails to localize but the *Xcat*-2 3′UTR (E) localizes as efficiently as does the full-length sequence (B). (F) Oocyte injected with a DIG-labeled chimeric transcript containing the luciferase-tagged 3′UTR of *Xcat*-2. The 3′UTR is sufficient for mitochondrial cloud localization. Note however that the 400 nt luciferase tag is not as efficiently localized or retained in the cloud as the smaller transcripts and this is reflected in the higher background levels. Arrowheads indicate the mitochondrial cloud. The anti-DIG antibody non-specifically reacts with nucleoli (also seen in Fig. 1F). See Fig. 4 for schematic of the constructs used to generate the injected *Xcat*-2 transcripts and for quantitation of localization results. Bar, 80 µm.
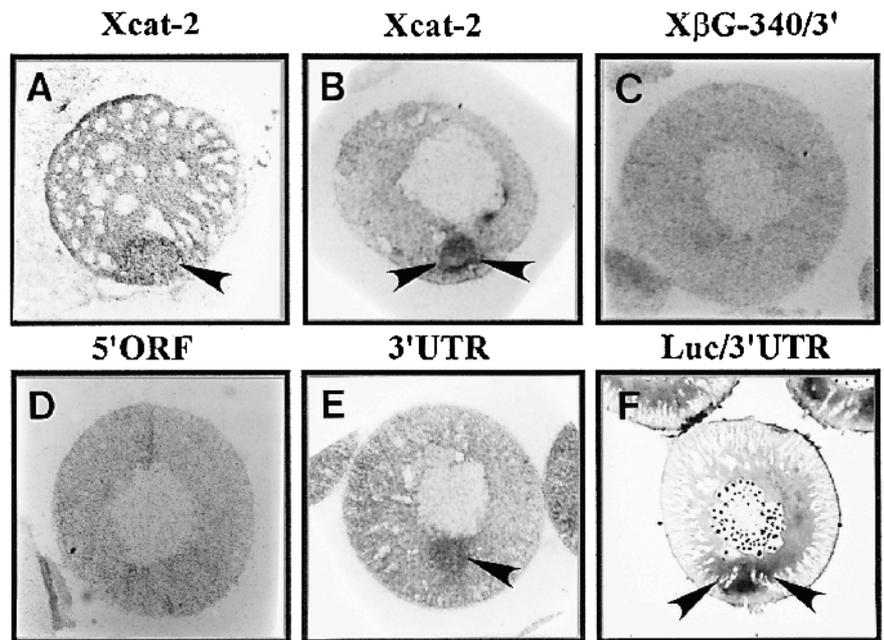
mitochondrial cloud localization signal, the 5′ORF and the 3′UTR deletion mutants of *Xcat*-2 were tested. Examples of injected oocytes are presented in Fig. 3 and quantitation of the results is presented in Fig. 4. The 3′UTR of *Xcat*-2 alone localized to the mitochondrial cloud 91% of the time (Fig. 3E) while the 5′ORF failed to do so in a 100% of the cases (Figs 3D, 4). To test for sufficiency of the 3′UTR in localization, 400 nt of the luciferase-coding region was fused to this region and the chimeric transcript introduced into stage 1 oocytes. In this instance, the transcript was detected by in situ hybridization using a DIG-labelled antisense luciferase probe. The luciferase-tagged transcript localized to the cloud in 74% of the cases and within the same time period as full-length *Xcat*-2, arguing that the 3′UTR was not only required but sufficient for localization (Fig. 3F). It is also clear from this analysis that prior translation of an exogenous, injected *Xcat*-2 is not required for correct localization.

In order to locate the minimum sequence in the 3′UTR required for mitochondrial cloud localization, four different deletion mutants were tested that divided this region into three parts: proximal, middle and distal (Fig. 4). The only deletion tolerated was of the distal half (3′UTRΔ1 in Fig. 4). The 3′UTRΔ2, 3′UTRΔ3 and 3′UTRΔ4 mutants all failed to localize. From this, we conclude that the proximal 250 nt are required for mitochondrial cloud targeting. The minimal localization signal sufficient to target ectopically introduced *Xcat*-2 to just the vegetal cortex in stage IV oocytes has been mapped (Zhou and King, 1996). Again, the 3′UTRΔ2 and 3′UTRΔ4 mutants lack localization

activity. However, whereas the mitochondrial cloud signal is broken by the *Bcl*I site in the 3′UTRΔ3 mutant, this mutant can localize to the vegetal cortex (Zhou and King, 1996). Therefore, there appear to be two localization elements within the 3′UTR with the mitochondrial cloud element larger and inclusive of part of the vegetal cortex localization signal.

Name of constructs	Map of constructs	% Mitochondrial cloud localization				
		−	+	++	(n)	Total % Localized
Xcat-2		19	56	25	(16)	81
5'ORF		100	0	0	(43*)	0
3'UTR		9	68	23	(22)	91
3'UTRΔ1		5	21	74	(19)	95
3'UTRΔ2		100	0	0	(35)	0
3'UTRΔ3		91	9	0	(23)	9
3'UTRΔ4		100	0	0	(26)	0
Luc/3'UTR		26	47	27	(15)	74

(Map labels: DdeI 455, BstNI 470, BclI 613, SmaI 692, ApaI 760)

Fig. 4. The localization element maps to a 250 nt region within the 3′UTR. Deletion mutations used to create mutant transcripts are shown in schematic form. The *Xcat*-2 ORF (shaded) and the 3′UTR (black) of *Xcat*-2 are shown. Deletions within the 3′UTR are indicated by interruptions in the black lines. 50 bp of the 5′ leader sequence of *Xenopus* β-globin cDNA (open box) or 400 bp of the luciferase-coding region (slanted lines) was used to tag the *Xcat*-2 3′UTR. Mitochondrial cloud localization was detected by autoradiography (for globin-tagged ^{35}S-labeled *Xcat*-2) or in situ hybridization (for luciferase-tagged *Xcat*-2) with DIG-labeled probes. Localization of the encoded transcripts in stage I was scored as minus as shown in Fig. 3C or D; plus (signal was 2-fold or 4-fold over background) as represented in Fig. 3A, or plus plus (signal was >5-fold over background) as shown in Fig. 3B. Silver grains over the mitochondrial cloud and an equal area over the nucleus (background) were counted. Only oocytes with obvious mitochondrial clouds were scored (n) except for the 5′ORF construct (*) as the uniform signal made detection of the cloud difficult in this case. Data are based on two series of injections.

DISCUSSION

In this work, we have examined *Xcat*-2 RNA localization to the mitochondrial cloud in stage I oocytes. We find that the mechanism for localization is distinctly different from that which has been described for *Vg*1 transport to the vegetal cortex in stage III/IV oocytes. In the case of *Vg*1, current evidence strongly supports directed transport as the mechanism involved (Yisraeli et al., 1990). Uniformly distributed *Vg*1 is moved by means of microtubules to a perinuclear position and is then again transported by microtubules to the vegetal cortex (Yisraeli et al., 1990; Forristall et al., 1995; Zhou and King, 1996). In contrast, results presented here are most consistent with the mitochondrial cloud containing specific binding sites that sequester *Xcat*-2 RNA to this location. Injected *Xcat*-2 RNA gradually accumulates within the cloud with no intermediate steps involving concentration gradients or perinuclear localization. Background levels of *Xcat*-2 remained uniform in the ooplasm over the course of localization. Since stage I oocytes are relatively small and yolk platelets have not yet formed in the ooplasm, diffusion alone may be sufficient to provide the necessary binding opportunities for *Xcat*-2 to concentrate within the large mitochondrial cloud. These binding sites must be RNA and region specific as *Vg*1 cannot bind to the mitochondrial cloud and *Xcat*-2 does not concentrate within the other mitochondrial aggregates arrayed around the nucleus, but only accumulates within the cloud. However, although the pattern of localization is most consistent with a model of localized binding sites, we cannot yet rule out a role for microtubules.

Two other possible mechanisms for localization have been described by St Johnston (1995): selective degradation (Ding et al., 1993) and vectorial nuclear transport (Davis and Ish-Horowicz, 1991). Vectorial nuclear export as a possible mechanism seems unlikely since *Xcat*-2 RNA was found uniformly distributed in the ooplasm of early stage I oocytes and only later entered the cloud. Selective degradation as a model is also unlikely as *Xcat*-2 RNA levels remain constant during oogenesis and actually increase during stage I (Fig. 2). Furthermore, injected *Xcat*-2 concentrated within the mitochondrial cloud without significant degradation as indicated by the lack of recycled label appearing in the nucleus (Fig. 3B). In fact, the *Xcat*-2 signal within the mitochondrial cloud appeared to increase as the signal found in the general ooplasm declined. Both these observations argue against selective degradation as a mechanism for localization where only the *Xcat*-2 in the cloud remains intact.

One general concept that has emerged from studies on RNA localization, irrespective of the organism, cell type or mechanism involved, is that the signal for localization (RLS) resides in the 3′UTR (Macdonald and Struhl, 1988; Kim-Ha et al., 1991; Mowry and Melton, 1992; Kloc et al., 1993). The results of fine deletion mapping of the *bicoid* (MacDonald et al., 1993; Ferrandon et al., 1994), *oskar* (Kim-Ha et al., 1991) and actin (Kislauskis et al., 1994) RLSs suggest that the large signal may consist of several smaller elements with different elements responsible for distinct steps in the localization pathway. Analysis of *Xcat*-2 deletion mutants indicated that a 250 nt region upstream of the *Sma*I site in the 3′UTR of *Xcat*-2 is required for mitochondrial cloud localization. All localization activity was lost in the 3′UTRΔ3 mutant in which this region is broken. Interestingly, in related but separate experiments, the 3′UTRΔ3 mutant was both required and sufficient to target *Xcat*-2 to the vegetal cortex in stage IV oocytes (Zhou and King, 1996). Since the signal sufficient for vegetal cortical localization in *Xcat*-2 (3′UTRΔ3) and *Vg*1 (XβG-340/3′) fails to localize to the mitochondrial cloud when tested in stage I oocytes, our results define two elements in the *Xcat*-2 3′UTR that have different functions or binding abilities. The localization requirements for the mitochondrial cloud may require additional and/or different RNA-protein interactions compared to vegetal cortical localization. These differences in RNA *cis*-localization signals could also underlie the different cortical binding properties that have been observed for *Xcat*-2 and *Vg*1 (Forristall et al., 1995; King, 1995; Kloc and Etkin, 1994).

The mitochondrial cloud appears to contain binding sites for a number of RNAs in addition to *Xcat*-2. These include *Xlsirts* (Kloc et al., 1993; Kloc and Etkin, 1994) and *Xwnt*-11 (Ku and Melton, 1993). We have isolated an additional four RNAs that all localize to the mitochondrial cloud bringing the total to seven. These new mitochondrial cloud RNAs will be reported on elsewhere (King, 1995; Zhang and King, unpublished). *Xlsirts* are non-coding RNAs that may play a role in RNA binding to the vegetal cortex (Kloc and Etkin, 1994). *Xwnt*-11 is a member of the Wnt-family of growth factors and its protein can partially rescue a dorsal axis in UV-irradiated embryos (Ku and Melton, 1993). No localization elements for *Xwnt*-11 have been mapped yet, but, when we compared the 250 nt mitochondrial cloud localization signal in *Xcat*-2 with the 3′UTR of *Xwnt*-11, we could not find any significant homologies. However, it is difficult to prove that similarities in RNA sequence or secondary structure are significant without further mutant analysis.

What is the underlying purpose of localizing mRNAs to the mitochondrial cloud? Heasman et al. (1984) have suggested that one of the important functions of the mitochondrial cloud is to accumulate and localize germ plasm to the vegetal pole. We have previously shown that *Xcat*-2 appears to be a component of the germ plasm (Forristall et al., 1995) and two other mitochondrial cloud RNAs that we have isolated co-localize with *Xcat*-2 (Zhang and King, unpublished). It is well known that primordial germ cells must lie in the endoderm to migrate properly into the developing gonads (Wylie et al., 1985b). In *Drosophila* the genetic pathway that specifies the PGC lineage is linked to that which specifies abdomen, the correct position for PGC development in flies (Lehmann and Ephrussi, 1994). In an analogous fashion, the genetic pathway that specifies the PGCs may be linked to that which specifies endodermal fate in frogs. The physical link could be the co-localization of determinants to the vegetal cortex by means of the mitochondrial cloud. If this is true, we would predict that mRNAs involved in specifying dorsal and/or endoderm would also be found in the mitochondrial cloud. *Xwnt*-11 would be a candidate for such an RNA.

The overlap in localization signals between the early and late pathways revealed by the deletion mutant analysis of *Xcat*-2 may also be significant. Perhaps the early pathway evolved from the late one as a specialized transport system for localizing germ plasm material early, before the localization of most other RNAs involved in somatic cell differentiation like *Vg*1. It is interesting to speculate that the posterior pole of *Drosophila* and the vegetal pole of *Xenopus*, both sites where the germ cell determinants become localized, localize some RNAs using a similar mechanism. In this regard, *nanos*, *cyclin* B and *germ cell-less* mRNAs are thought to accumulate at the

posterior pole because of specific binding sites localized in this domain (Wang et al., 1994; Raff et al., 1990). Clearly, the mechanism that targets RNAs to the mitochondrial cloud plays an important role in establishing polarity in the oocyte and, as a consequence, cell fate in the embryo.

REFERENCES

Bassez, T., Paris, J., Omilli, F., Dorel, C. and Osborne, H. B. (1990). Post-transcriptional regulation of ornithine decarboxylase in *Xenopus* oocytes. *Development* **110**, 955-962.

Billett, F. S. and Adam, E. (1976). The structure of the mitochondrial cloud of *Xenopus laevis* oocytes. *J. Embryol. Exp. Morph.* **33**, 697-710.

Davis, I. and Ish-Horowicz, D. (1991). Apical localization of pair-rule transcripts requires 3′ sequences and limits protein diffusion in the *Drosophila* blastoderm embryo. *Cell* **67**, 927-940.

Ding, D., Parkhurst, S. M., Halsell, S. R. and Lipshitz, H. D. (1993). Dynamic hsp83 RNA localization during *Drosophila* oogenesis and embryogenesis. *Mol. Cell. Biol.* **13**, 3773-3781.

Dumont, J. N. (1972). Oogenesis in *Xenopus laevis* (Daudin). I. Stage of oocyte development in laboratory maintained animals. *J. Morph.* **136**, 153-180.

Ferrandon, D., Elphick, L., Nusslein-Volhard, C. and St. Johnston, D. (1994). Staufen protein associates with the 3′UTR of *bicoid* mRNA to form particles that move in a microtubule-dependent manner. *Cell* **79**, 1221-1232.

Forristall, C., Pondel, M., Chen, L. and King, M. L. (1995). Patterns of localization and cytoskeletal association of two vegetally localized RNAs, *Vg*1 and *Xcat*-2. *Development* **121**, 201-208.

Gard, D. L., Affleck, D. and Error, B. M. (1995). Microtubule Organization, Acetylation, and Nucleation in *Xenopus laevis* oocytes: II. A developmental transition in microtubule organization during early diplotene. *Dev. Biol.* **168**, 189-201.

Genetics Computer Group Inc. (1992). *GCG Program Manual Version* 8.0

Gurdon, J. (1968). Changes in somatic cell nuclei inserted into growing and maturing amphibian oocytes. *J. Embryol. Exp. Morph.* **20**, 401-414.

Harland, R. M. (1991). In *Methods in Cell Biology*, vol. 6, (ed. B. P. Kay and H. B. Peng). pp. 685-695. San Diego, California: Academic Press.

Hausen, P. and Riebesell, M. (1991). *The Early Development of* Xenopus laevis. New York: Springer-Verlag.

Heasman, J., Quarmby, J. and Wylie, C. C. (1984). The mitochondrial cloud of *Xenopus* oocytes: The source of germinal granule material. *Dev. Biol.* **105**, 458-469.

Ikenishi, K., Nakazato, S. and Okuda, T. (1986). Direct Evidence for the presence of germ cell determinant in vegetal pole cytoplasm of *Xenopus laevis* and in a subcellular fraction of it. *Develop. Growth and Differ.* **28**, 563-568.

Kim-Ha, J., Smith, J. L. and MacDonald, P. M. (1991). *oskar* mRNA id localized to the posterior pole of the *Drosophila* oocyte. *Cell* **66**, 23-35.

Kim-Ha, J., Webster, P. J., Smith, J. L. and MacDonald, P. M. (1993). Multiple RNA regulatory elements mediate distinct steps in localization of *oskar* mRNA. *Development* **119**, 169-178.

King, M. L. (1995). mRNA localization during frog oogenesis. In *Localized RNAs; Molecular Biology Intelligence Unit.* (ed. H. Lipshitz). pp. 137-148. Austin, TX: R. G. Landes Company of Biomedical Publishers.

Kislauskis, E. H., Zhu, X. and Singer, R. H. (1994). Sequences responsible for intracellular localization of β-actin messenger RNA also affect cell phenotype. *J. Cell Biol.* **127**, 441-451.

Kloc, M., Sophr, G. and Etkin, L. D. (1993). Translocation of repetitive RNA sequences with the germ plasm in *Xenopus* oocytes. *Science* **262**, 1712-1714.

Kloc, M. and Etkin, L. D. (1994). Delocalization of *Vg*1 mRNA from the vegetal cortex in *Xenopus* oocytes after destruction of *Xlsirt* RNA. *Science* **265**, 1101-1103.

Kloc, M. and Etkin, L. D. (1995). Two distinct pathways for the localization of RNAs at the vegetal cortex in *Xenopus* oocytes. *Development* **121**, 287-297.

Kobayashi, S., Yamada, M., Asaoka, M. and Kitamura, T. (1996). Essential role of the posterior morphogen nanos for germline development in *Drosophila*. *Nature* **380**, 708-711.

Krieg, P. A. and Melton, D. A. (1984). Functional messenger RNAs are produced by SP6 in vitro transcription of cloned cDNAs. *Nucl. Acid Res.* **12**, 7057-7070.

Ku, M. and Melton, D. A. (1993). *Xwnt-11*: a maternally expressed *Xenopus wnt* gent. *Development* **119**, 1161-1173.

Lehmann, R. and Ephrussi, A. (1994). Germ plasm formation and germ cell determination in *Drosophila*. *Ciba Found. Symp.* **182**, 282-296.

Lehmann, R. and Nusslein-Volhard, C. (1991) The maternal gene *nanos* has a central role in posterior pattern formation of the *Drosophila* embryo. *Development* **112**, 679-691.

MacDonald, P. M. and Struhl, G. (1988). *Cis*-acting sequences responsible for anterior localization of *bicoid* mRNA in *Drosophila* embryos. *Nature* **336**, 595-598.

MacDonald, P. M., Kerr, K., Smith, J. L. and Leask, A. (1993) RNA regulatory element BLE1 directs the early steps of *bicoid* mRNA localization. *Development* **118**, 1233-1243.

Mahowald, A. P. and Hennen, S. (1971). Ultrastructure of the 'germ plasm' in eggs and embryos of *Rana pipiens*. *Dev. Biol.* **24**, 37-53.

Melton, D. A. (1987). Translocation of a localized maternal mRNA to the vegetal pole of *Xenopus* oocytes. *Nature* **328**, 80-82.

Melton, D. A., Krieg, P. A., Rebagliati, M. R., Maniatis, T., Zinn K. and Green, M. R. (1984). Efficient *in vitro* synthesis of biologically active RNA and RNA hybridization probes from plasmids containing a bacteriophage SP6 promoter. *Nucl. Acids Res.* **12**, 7035-7056.

Mosquera, L., Forristall, C., Zhou, Y. and King, M. L. (1993). A mRNA localized to the vegetal cortex of *Xenopus* oocytes encodes a protein with a *nanos*-like zinc finger domain. *Development* **117**, 377-386.

Mowry, K. L. and Melton, D. A. (1992). Vegetal messenger RNA localization directed by a 340 nt RNA sequence element in *Xenopus* oocytes. *Science* **255**, 991-994.

Oberman, F. and Yisraeli, J. K. (1995). Two non-radioactive techniques for in situ hybridzation to *Xenopus* oocytes. *Trends in Genetics* **11**, 83-84.

Peng, H. B. (1991). Appendix A. Solutions and protocols. In *Methods in Cell Biology vol. 36., Xenopus laevis: Practical uses in Cell and Molecular Biology* (ed. B. K. Kay and H. B. Peng). pp. 659. San Diego, California: Academic Press, Inc.

Rabagliati, M. R., Weeks, D. L., Harvey, R. P. and Melton, D. A. (1985) Identification and cloning of localized maternal RNAs from *Xenopus* eggs. *Cell* 42, 769-777.

Raff, J. W., Whittlefield, W. G. F. and Glover, D. M. (1990). Two distinct mechanisms localize cyclin B transcripts in syncytial *Drosophila* embryos. *Development* **120**, 1233-1242.

Rusconi, C. and Flick, P. K. (1993). A comparison of the RNA tailing activities of cloned Yeast poly(A) polymerase and E. coli poly(A) polymerase. *Editorial Comments (USB)* 20(2), 35-36.

St. Johnston, D. (1995). The intracellular localization of messenger RNAs. *Cell* **81**, 161-170.

Tourte, M., Mignotte, F. and Mounolou, J. C. (1984). Heterogenous distribution and replication activity of mitochondria in *Xenopus laevis* oocytes. *Eur. J. Cell Biol.* **34**, 171-178.

Wallace, R. A., Misulovin, Z. and Wiley, H. S. (1980). Growth of anuran oocytes in serum-supplemented medium. *Reprod. Nutr. Dev.* **20**, 699-708.

Wang, C., Dickinson, L. K. and Lehmann, R. (1994). Genetics of *nanos* localization in *Drosophila*. *Dev. Dyn.* **199**, 103-115.

Wylie, C. C., Brown, D., Godsave, S. F., Quarmby, J. and Heasman, J. (1985a). The cytoskeleton of *Xenopus* oocytes and its role in development. *J. Embryol. Exp. Morph.* **89 Supplement**, 1-15.

Wylie, C. C., Heasman, H., Snape, A., O'Driscoll, M. and Holwill, S. (1985b). Primordial Germ Cells of *Xenopus laevis* are not irreversibly determined early in development. *Dev. Biol.* **112**, 66-72.

Yisraeli, J. K. and Melton, D. A. (1988). The maternal mRNA *Vg*1 is correctly localized following injection into *Xenopus* oocytes. *Nature* **336**, 592-595

Yisraeli, J. K., Sokol, S. and Melton, D. A. (1990). A two-step model for the localization of maternal mRNA in *Xenopus* oocytes: involvement of microtubules and microfilaments in the translocation and anchoring of *Vg*1 mRNA. *Development* **108**, 289-298.

Yost, H. J., Phillips, C. R., Boore, J. L., Bertman, J., Whalon, B. and Danilchik, M. V. (1995). Relocation of mitochondria to the prospective dorsal marginal zone during *Xenopus* embryogenesis. *Dev. Biol.* **170**, 83-90.

Zhou, Y. and King, M. L. (1996). RNA transport to the vegetal cortex of *Xenopus* oocytes. *Dev. Biol.* In press.

Zuker, M. (1989). On finding all suboptimal foldings of an RNA molecule. *Science* **244**, 48-52.